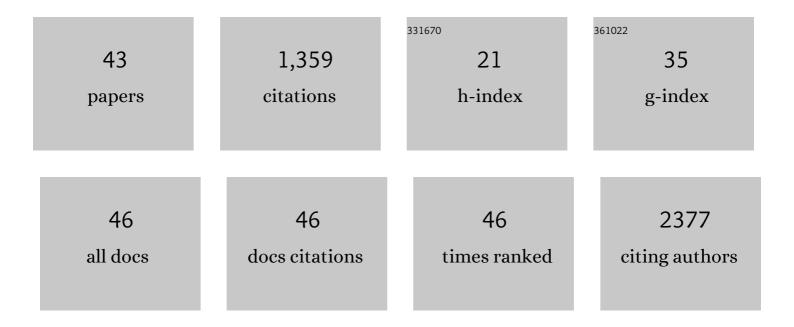
## Wayne F Anderson

List of Publications by Year in descending order

Source: https://exaly.com/author-pdf/9183455/publications.pdf Version: 2024-02-01



#	Article	IF	CITATIONS
1	Sensor Domain of Histidine Kinase VxrA of Vibrio cholerae: Hairpin-Swapped Dimer and Its Conformational Change. Journal of Bacteriology, 2021, 203, .	2.2	4
2	A comparative genomics approach identifies contact-dependent growth inhibition as a virulence determinant. Proceedings of the National Academy of Sciences of the United States of America, 2020, 117, 6811-6821.	7.1	39
3	A Selective and Brain Penetrant p38αMAPK Inhibitor Candidate for Neurologic and Neuropsychiatric Disorders That Attenuates Neuroinflammation and Cognitive Dysfunction. Journal of Medicinal Chemistry, 2019, 62, 5298-5311.	6.4	31
4	Analysis of crystalline and solution states of ligand-free spermidine <i>N</i> -acetyltransferase (SpeG) from <i>Escherichia coli</i> . Acta Crystallographica Section D: Structural Biology, 2019, 75, 545-553.	2.3	8
5	Structural Basis for DNA Recognition by the Two-Component Response Regulator RcsB. MBio, 2018, 9, .	4.1	15
6	Structure of the Bacillus anthracis dTDP- l -rhamnose biosynthetic pathway enzyme: dTDP-α- d -glucose 4,6-dehydratase, RfbB. Journal of Structural Biology, 2018, 202, 175-181.	2.8	8
7	An acetylatable lysine controls CRP function in <i>E. coli</i> . Molecular Microbiology, 2018, 107, 116-131.	2.5	51
8	The spermidine acetyltransferase SpeG regulates transcription of the small RNA rprA. PLoS ONE, 2018, 13, e0207563.	2.5	4
9	The bacterial Ras/Rap1 site-specific endopeptidase RRSP cleaves Ras through an atypical mechanism to disrupt Ras-ERK signaling. Science Signaling, 2018, 11, .	3.6	39
10	CSGID Solves Structures and Identifies Phenotypes for Five Enzymes in Toxoplasma gondii. Frontiers in Cellular and Infection Microbiology, 2018, 8, 352.	3.9	14
11	Listeria monocytogenes InlP interacts with afadin and facilitates basement membrane crossing. PLoS Pathogens, 2018, 14, e1007094.	4.7	35
12	Structural and immunological characterization of <i>E. coli</i> derived recombinant CRM197 protein used as carrier in conjugate vaccines. Bioscience Reports, 2018, 38, .	2.4	23
13	Transferase Versus Hydrolase: The Role of Conformational Flexibility in Reaction Specificity. Structure, 2017, 25, 295-304.	3.3	23
14	Identification of novel small molecule inhibitors against NS2B/NS3 serine protease from Zika virus. Antiviral Research, 2017, 139, 49-58.	4.1	113
15	Insight into the 3D structure and substrate specificity of previously uncharacterized GNAT superfamily acetyltransferases from pathogenic bacteria. Biochimica Et Biophysica Acta - Proteins and Proteomics, 2017, 1865, 55-64.	2.3	13
16	Structure to function of an α-glucan metabolic pathway that promotes Listeria monocytogenes pathogenesis. Nature Microbiology, 2017, 2, 16202.	13.3	33
17	Structure of the <i>Bacillus anthracis</i> dTDP- <scp>L</scp> -rhamnose-biosynthetic enzyme dTDP-4-dehydrorhamnose reductase (RfbD). Acta Crystallographica Section F, Structural Biology Communications, 2017, 73, 644-650.	0.8	6
18	New ligation independent cloning vectors for expression of recombinant proteins with a self-cleaving CPD/6xHis-tag. BMC Biotechnology, 2017, 17, 1.	3.3	42

## WAYNE F ANDERSON

#	Article	IF	CITATIONS
19	Structure of theBacillus anthracisdTDP-L-rhamnose-biosynthetic enzyme glucose-1-phosphate thymidylyltransferase (RfbA). Acta Crystallographica Section F, Structural Biology Communications, 2017, 73, 621-628.	0.8	2
20	Structure of the <i>Bacillus anthracis</i> dTDP- <scp>L</scp> -rhamnose-biosynthetic enzyme dTDP-4-dehydrorhamnose 3,5-epimerase (RfbC). Acta Crystallographica Section F, Structural Biology Communications, 2017, 73, 664-671.	0.8	6
21	Crystal structures of the transpeptidase domain of the Mycobacterium tuberculosis penicillinâ€binding protein PonA1 reveal potential mechanisms of antibiotic resistance. FEBS Journal, 2016, 283, 2206-2218.	4.7	18
22	Crystal Structures of the SpoIID Lytic Transglycosylases Essential for Bacterial Sporulation. Journal of Biological Chemistry, 2016, 291, 14915-14926.	3.4	15
23	Structure of the Essential <i>Mtb</i> FadD32 Enzyme: A Promising Drug Target for Treating Tuberculosis. ACS Infectious Diseases, 2016, 2, 579-591.	3.8	37
24	Small angle X-ray scattering data and structure factor fitting for the study of the quaternary structure of the spermidine N-acetyltransferase SpeG. Data in Brief, 2016, 6, 47-52.	1.0	3
25	Crystal structure of nonphosphorylated receiver domain of the stress response regulator RcsB from <i>Escherichia coli</i> . Protein Science, 2016, 25, 2216-2224.	7.6	9
26	Loop-to-helix transition in the structure of multidrug regulator AcrR at the entrance of the drug-binding cavity. Journal of Structural Biology, 2016, 194, 18-28.	2.8	12
27	An Unusual Cation-Binding Site and Distinct Domain–Domain Interactions Distinguish Class II Enolpyruvylshikimate-3-phosphate Synthases. Biochemistry, 2016, 55, 1239-1245.	2.5	18
28	Fluorescence-based thermal shift data on multidrug regulator AcrR from Salmonella enterica subsp. entrica serovar Typhimurium str. LT2. Data in Brief, 2016, 7, 537-539.	1.0	0
29	Substrate-Induced Allosteric Change in the Quaternary Structure of the Spermidine N-Acetyltransferase SpeG. Journal of Molecular Biology, 2015, 427, 3538-3553.	4.2	12
30	A Novel Phosphatidylinositol 4,5-Bisphosphate Binding Domain Mediates Plasma Membrane Localization of ExoU and Other Patatin-like Phospholipases. Journal of Biological Chemistry, 2015, 290, 2919-2937.	3.4	34
31	Targeting Human Central Nervous System Protein Kinases: An Isoform Selective p38αMAPK Inhibitor That Attenuates Disease Progression in Alzheimer's Disease Mouse Models. ACS Chemical Neuroscience, 2015, 6, 666-680.	3.5	75
32	Structural Genomics Support for Infectious Disease Drug Design. ACS Infectious Diseases, 2015, 1, 127-129.	3.8	2
33	A Novel Polyamine Allosteric Site of SpeG from Vibrio cholerae Is Revealed by Its Dodecameric Structure. Journal of Molecular Biology, 2015, 427, 1316-1334.	4.2	24
34	Structural and functional analysis of betaine aldehyde dehydrogenase from <i>Staphylococcus aureus</i> . Acta Crystallographica Section D: Biological Crystallography, 2015, 71, 1159-1175.	2.5	16
35	Discovery of Selective Inhibitors of the Clostridium difficile Dehydroquinate Dehydratase. PLoS ONE, 2014, 9, e89356.	2.5	12
36	Structural, Kinetic and Proteomic Characterization of Acetyl Phosphate-Dependent Bacterial Protein Acetylation. PLoS ONE, 2014, 9, e94816.	2.5	249

WAYNE F ANDERSON

#	Article	IF	CITATIONS
37	Potential for Reduction of Streptogramin A Resistance Revealed by Structural Analysis of Acetyltransferase VatA. Antimicrobial Agents and Chemotherapy, 2014, 58, 7083-7092.	3.2	19
38	Structure-Based Mutational Studies of Substrate Inhibition of Betaine Aldehyde Dehydrogenase BetB from Staphylococcus aureus. Applied and Environmental Microbiology, 2014, 80, 3992-4002.	3.1	52
39	Structure of the LdcB LD-Carboxypeptidase Reveals the Molecular Basis of Peptidoglycan Recognition. Structure, 2014, 22, 949-960.	3.3	31
40	Structural, Functional, and Inhibition Studies of a Gcn5-related N-Acetyltransferase (GNAT) Superfamily Protein PA4794. Journal of Biological Chemistry, 2013, 288, 30223-30235.	3.4	37
41	Development of Novel In Vivo Chemical Probes to Address CNS Protein Kinase Involvement in Synaptic Dysfunction. PLoS ONE, 2013, 8, e66226.	2.5	58
42	The structure of the <i>yrdC</i> gene product from <i>Escherichia coli</i> reveals a new fold and suggests a role in RNA binding. Protein Science, 2000, 9, 2557-2566.	7.6	74
43	Structure of the fibrinogen γâ€chain integrin binding and factor XIIIa crossâ€linking sites obtained through carrier protein driven crystallization. Protein Science, 1999, 8, 2663-2671.	7.6	39